Assessment of Malignant Pleural Mesothelioma with ^{18}F-FDG Dual-Head Gamma-Camera Coincidence Imaging: Comparison with Histopathology

Victor H. Gerbaudo, PhD[1]; David J. Sugarbaker, MD[2]; Scott Britz-Cunningham, MD, PhD[1]; Marcelo F. Di Carli, MD[1]; Charles Mauceri[1]; and S. Ted Treves, MD[1]

[1]Division of Nuclear Medicine, Department of Radiology, Brigham and Women's Hospital and Harvard Medical School, Boston, Massachusetts; and [2]Division of Thoracic Surgery, Department of Surgery, Brigham and Women's Hospital and Harvard Medical School, Boston, Massachusetts

Malignant pleural mesothelioma is an aggressive primary neoplasm for which early detection and accurate staging are known diagnostic challenges. The role of ^{18}F-FDG dual-head gamma-camera coincidence imaging (^{18}F-FDG-CI) is yet to be defined. The purpose of this study was to evaluate the usefulness of ^{18}F-FDG-CI in the assessment of malignant pleural mesothelioma using histopathology as the gold standard. **Methods:** Fifteen consecutive patients with CT scan evidence of pleural thickening, fluid, plaques, or calcification underwent ^{18}F-FDG imaging 1.5 h after the intravenous administration of 370 MBq ^{18}F-FDG. Imaging was performed with a dual-head gamma camera equipped with 2.54-cm-thick NaI crystals operating in coincidence mode. Using an iterative algorithm, whole-body images were reconstructed as transaxial, sagittal, and coronal images. No attenuation correction was applied. The results of ^{18}F-FDG-CI scans were compared with CT and with histopathologic diagnosis. **Results**: Eleven of 15 patients had histologically proven malignant mesotheliomas (10 epithelial, 1 sarcomatoid). All 11 primary tumors were detected by ^{18}F-FDG, and absence of disease was confirmed in the 4 patients who were disease free. Thirty-four lesions were biopsied; among these, 29 were found to be positive for tumor. ^{18}F-FDG was true-positive in 28 lesions, true-negative in 4, false-negative in 1 (0.5 cm in diameter), and false-positive in 1 (inflammatory pleuritis). The smallest lesion detected was 0.8 cm. For biopsied lesions, overall sensitivity, specificity, and accuracy for ^{18}F-FDG-CI were 97%, 80%, and 94% respectively, compared with 83%, 80%, and 82% for CT. Twenty-one of 29 positive lesions involved the pleura, lung parenchyma, or chest wall and were all ^{18}F-FDG avid. In the mediastinum, ^{18}F-FDG-CI detected 7 of 8 biopsy-positive lesions (88%), whereas CT was positive in 6 of 8 lesions (75%). ^{18}F-FDG identified extrathoracic metastases in 5 patients, excluding them from surgical therapy. **Conclusion:** These preliminary results suggest that ^{18}F-FDG-CI appears to be an accurate method to diagnose and to define the extent of disease in patients with diffuse malignant pleural mesothelioma.

Key Words: ^{18}F-FDG; mesothelioma; coincidence imaging; pleural malignancies

J Nucl Med 2002; 43:1144–1149

Malignant pleural mesothelioma is a rare primary neoplasm, with an estimated annual incidence of approximately 7–13 per million white males in the United States (*1*). Its aggressive invasive behavior manifests itself by a median survival rate of between 4 and 12 mo (*2*). Survival has been shown to improve after the introduction of multimodality therapy schemes. Sugarbaker et al. (*2*) showed that median survival in these patients improves from 12 to 21 mo after early diagnosis, proper staging, and trimodality therapy (extrapleural pneumonectomy, followed by chemotherapy and radiation).

Early detection and accurate staging, however, are still known diagnostic challenges. Malignant pleural mesothelioma is an aggressive primary tumor characterized by local invasion of the pleural space followed by spread to intrathoracic and extrathoracic organs. In patients with suspicion of pleural malignancy there is a need for a reliable distinction between a benign and a malignant process as well as for the differentiation between focal or multifocal invasive disease. Under the Brigham and Women's Hospital surgical staging criteria, diffuse malignant mesothelioma is considered unresectable when there is local extension of the tumor into the mediastinal structures or across the diaphragm (*3*).

Although anatomic imaging modalities are successful at predicting tumor resectability, they have limitations when attempting to characterize pleural and mediastinal lesions as benign or malignant (*4*,*5*). The typical CT findings of diffuse pleural thickening and effusion are not specific for malignancy, and mediastinal nodes of <1 cm may harbor

Received Feb. 4, 2002; revision accepted May 17, 2002.

For correspondence or reprints contact: Victor H. Gerbaudo, PhD, Division of Nuclear Medicine, Department of Radiology, Brigham and Women's Hospital, 75 Francis St., Boston, MA 02115.

E-mail: vgerbaudo@bics.bwh.harvard.edu

micrometastatic foci, whereas nodes of >1 cm could represent reactive lymphadenitis. Cytologic examination of pleural fluid obtained by thoracentesis is relatively insensitive, and in most cases a pleural biopsy is necessary to reach the diagnosis. Closed pleural biopsy often leads to negative or inaccurate results because of inadequate sampling (*3*). This procedure proves to be useful only if findings are positive; therefore, definite diagnosis and staging typically rely on a surgical approach, by either open biopsy or thoracoscopy (*6*).

A limited number of encouraging reports address the use of ^{18}F-FDG and full-ring PET for the metabolic assessment of malignant mesothelioma (*7–10*). ^{18}F-FDG PET has been shown to be an accurate metabolic marker of malignancy in this setting and a sensitive method to assess the extent of disease. However, the role of ^{18}F-FDG dual-head gamma-camera coincidence imaging (^{18}F-FDG-CI) of mesothelioma is yet to be defined. Therefore, we sought to examine both the diagnostic accuracy of ^{18}F-FDG-CI and its role in the assessment of the disease extent in patients with malignant pleural mesothelioma. Results were compared with those obtained using CT and with histopathologic diagnosis, which served as the external reference standard.

MATERIALS AND METHODS

Patients

^{18}F-FDG-CI was performed on 15 patients (11 men, 4 women; mean age, 60 y; range, 37–74 y) with clinical and radiographic suspicion of malignant mesothelioma. In 9 of these patients, the ^{18}F-FDG-CI scan was obtained during their initial clinical evaluation to determine the presence of malignancy and the extent of disease. In the other 6 patients, scanning was performed to evaluate for tumor recurrence.

These patients typically presented with chest pain, shortness of breath, chronic cough, and shoulder or arm pain. Systemic symptoms included sweating, fever of unknown origin, and weight loss with declining performance status. Physical examination usually showed unilateral loss of breath sounds on auscultation and dullness on percussion. Typical findings on radiographic and CT studies included pleural effusion, atelectasis, nodular thickening of the pleura, pleural calcification, or an intrathoracic mass.

CT Imaging

CT scanning was performed with a multidetector row CT scanner (Somatom VolumeZoom; Siemens, Forchheim, Germany). Images were obtained from the lung apices to the upper abdomen with 1-mm collimation. Contiguous 5-mm slices were obtained during the intravenous administration of 100 mL of nonionic contrast material at 3 mL/s. CT scans always preceded ^{18}F-FDG imaging with a time interval of 2 ± 1 d.

^{18}F-FDG-CI

After fasting for at least 6 h, capillary blood glucose levels were measured on all patients. Mean serum glucose levels were 107 ± 21 mg/dL (range, 90–159 mg/dL). After the intravenous administration of 375.5 ± 19.6 MBq (10.15 ± 0.53 mCi) ^{18}F-FDG, patients rested for 90 min before imaging to minimize radiotracer muscle uptake. In our experience and that of others (*7*), longer intervals between injection and imaging have improved the image quality and the rate of tumor detection in the setting of pleural malignancies. Patients were encouraged to void before imaging, and whole-body scans were obtained starting in the pelvic area to minimize deterioration of image quality due to ^{18}F-FDG accumulation in the bladder over time. Scanning was performed with a dual-detector gamma camera (ECAM Duet; Siemens Medical Systems, Inc., Hoffman Estates, IL) equipped with 2.54-cm-thick NaI crystals and 2-dimensional axial shields, operating in coincidence mode. The axial field of view was 38 cm and all patients were scanned from the proximal thighs to the base of the skull in 2 bed positions. The analyzer was set with a single 30% window centered around the 511-keV photopeak for ^{18}F. Images were acquired for 64 projections (with a 128 × 128 matrix) at 25 s per stop through a circular orbit of 180° per detector. The total acquisition time per bed position was approximately 27 min, and decay correction was applied. The intrinsic resolution was ≤5.3-mm full width at half maximum (FWHM) at the center, and the reconstructed resolution was 4.7-mm FWHM. The system's sensitivity with 2-dimensional axial shields was in the order of 30 kcps/37 kBq/mL (30 kcps/μCi/mL) (where kcps = kilocounts per second). The maximum single counting rate per detector was 2.0 Mcps. One hundred twenty-eight rebinned views were reconstructed using an ordered subset expectation maximization iterative algorithm (*11*). Reconstruction involved an order subset of 4 with 6 iterations followed by 3-dimensional smooth filtering. Random subtraction and axial normalization were performed. Images were not corrected for attenuation. Processed data were then displayed in the transaxial, sagittal, and coronal planes and displayed on the computer screen for interpretation.

Image Analysis

Image interpretation was visual and was performed separately by 2 experienced observers. Differences between them were resolved by consensus. A scan was considered positive by the presence of focal or linear, diffuse, or heterogeneous increased ^{18}F-FDG uptake compared with the normal surrounding background. The degree of hypermetabolic ^{18}F-FDG activity in each lesion was expressed semiquantitatively as follows: 0, absence of uptake; 1, low (less than liver uptake); 2, moderate (equal to liver uptake); and 3, high (higher than liver uptake). ^{18}F-FDG-CI results were compared with CT and with the final diagnosis provided by histopathology and immunohistochemistry used as the gold standards.

Histopathology

Within 1 wk of the completion of the imaging studies, specimens were obtained from needle biopsy, thoracoscopy, pleuroscopy, cytologic examination of pleural fluid, or mediastinoscopy. Tissue samples were also collected during pleurectomy or extrapleural pneumonectomy procedures. Morphologic diagnosis of mesothelioma was confirmed by immunohistochemical techniques. The following microscopic criteria were used to diagnose diffuse mesotheliomas (*12*): (a) epithelial type: characterized by tubulopapillary, tubuloglandular, lace-like, cleft-like, or cord-like patterns, and loss of cellular cohesion with polygonal or round cells distributed on a myxoid stroma or on the surface of mucinous pools; (b) fibrous or sarcomatoid type: a diffuse and pleomorphic spindle cell pattern, with occasional giant cells in areas of necrosis, hyalinization, and fibrosis; and (c) mixed or biphasic type: a mixture of sarcomatoid and epithelial components. Differentiation from adenocarcinoma, or from other primary or metastatic epithelial neoplasms, relied on a typical staining pattern (alcian blue, +;

periodic acid–Schiff-diastase, −) and immunohistochemical characteristics (cytokeratins: AE1/AE3, +; calretinin, +; and carcinoembryonic antigen, Leu-M1, and TTF-1, −).

Statistical Analysis

Data are presented as mean ± SD. Sensitivity, specificity, and accuracy of CT and ^{18}F-FDG-CI were calculated with the standard formulas. The degree of agreement between each imaging modality and biopsy results was quantified with the κ-statistic. $P < 0.05$ was used to define statistical significance.

RESULTS

Eleven of 15 patients had histologically proven diffuse malignant mesotheliomas. The cellular type was epithelial in 10 patients (90%) and sarcomatoid in 1 patient (10%).

All 11 patients with biopsy-proven mesothelioma had positive ^{18}F-FDG-CI scans, and the absence of disease was confirmed in the 4 patients who were tumor free (with histologic diagnoses of chronic fibrosing pleuritis in 2, chronic inflammatory response to talc pleurodesis in 1, and foreign body cell reaction in 1 patient with a history of asbestosis). Thirty-four lesions were biopsied; of these, 29 were found to be positive for tumor. ^{18}F-FDG-CI was true-positive in 28, true-negative in 4, false-negative in 1, and false-positive in 1. The smallest lesion detected was 0.8 cm. Overall sensitivity, specificity, and accuracy for ^{18}F-FDG-CI were 97% (95% confidence interval, 80%–99%), 80% (95% confidence interval, 30%–98%), and 94%, respectively, compared with 83% (95% confidence interval, 64%–93%), 80% (95% confidence interval, 30%–98%), and 82% for CT. ^{18}F-FDG-CI agreed with biopsy results in 94% of the evaluated lesions ($\kappa = 0.77$; $P < 0.0001$), whereas CT had an 82% agreement ($\kappa = 0.47$; $P < 0.003$).

Primary Tumors

Twenty-one lesions involved the pleura. Of these, 2 (9.5%) also affected the lung parenchyma and 3 (14%) affected the chest wall. Seventeen lesions were confirmed as malignant and all were ^{18}F-FDG avid. In the remaining 4 histologically benign lesions, ^{18}F-FDG-CI was true-negative in 3 and false-positive in 1. Three distinct patterns of ^{18}F-FDG uptake were observed: focal or linear, diffuse, and heterogeneous. These patterns of uptake matched the abnormalities and the extent of pleural and parenchymal involvement observed with anatomic imaging modalities (Fig. 1). Three patients had disease involving the chest wall, and ^{18}F-FDG-CI images correctly showed diffuse chest wall uptake with distortion of the thoracic contour in all 3 patients. In contrast, CT yielded false-negative results in 2 of these patients. ^{18}F-FDG-CI detected bilateral pleural disease in 3 patients, whereas CT failed to show contralateral involvement in 2 of these patients (Fig. 2). The intensity of uptake was higher in those lesions with the highest degree of pleomorphism and anaplasia, regardless of the histologic type. The only false-positive finding with ^{18}F-FDG-CI was an area of diffuse or low uptake in the right costophrenic sulcus of a patient who had been treated with talc pleurodesis due to recurrent, symptomatic pleural effusions.

Mediastinal Metastases

Mediastinal lymph node metastases were correctly identified by ^{18}F-FDG-CI in 6 patients with 8 histologically proven malignant lesions. The median lesion size was 1.65 cm (range, 0.5–4.5 cm). Focally increased uptake of ^{18}F-FDG was evident in 7 of 8 mediastinal lesions (88%), whereas CT was positive in 6 of 8 (75%). The source of the false-negative finding with ^{18}F-FDG-CI was a 0.5-cm right tracheobronchial node, which was also negative by CT. The second false-negative result on CT was a 1-cm right hilar node. CT yielded 1 false-positive finding of a 2-cm pretracheal node, which was histologically benign and non-^{18}F-FDG avid. In the remaining 5 patients with malignancy, ^{18}F-FDG-CI and CT were both negative in the mediastinum of 4 patients and positive in 1 patient; however, biopsy confirmation was not available in these patients. The patient

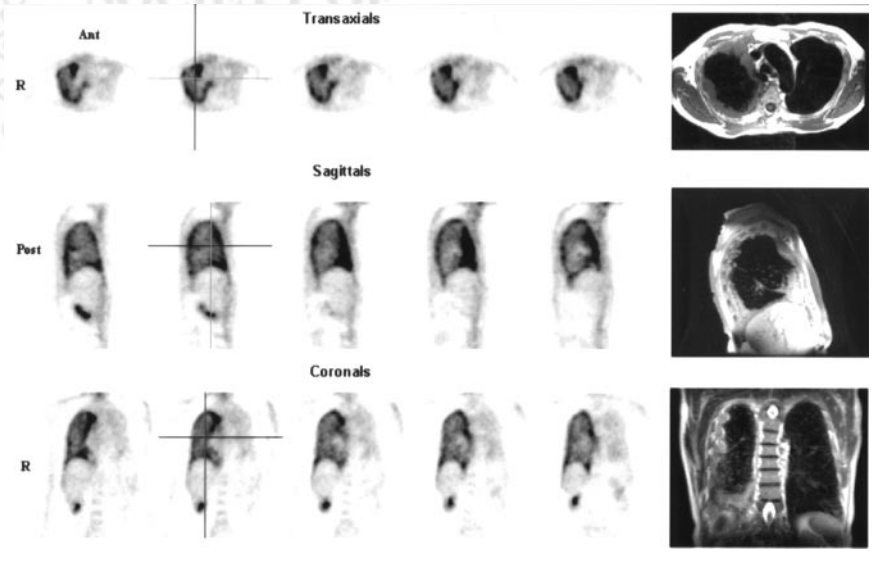

FIGURE 1. ^{18}F-FDG-CI and MRI images of patient with biopsy-confirmed epithelial-type malignant mesothelioma of right pleura. ^{18}F-FDG images show diffusely increased uptake of tracer along pleural space encasing right lung. Transaxial and sagittal images suggest involvement of anterior chest wall, with pleural uptake extending to right paracardiac mediastinum. ^{18}F-FDG-CI findings are in close agreement with extensive soft-tissue pleural mass seen on MRI. Ant = anterior; Post = posterior; R = right.

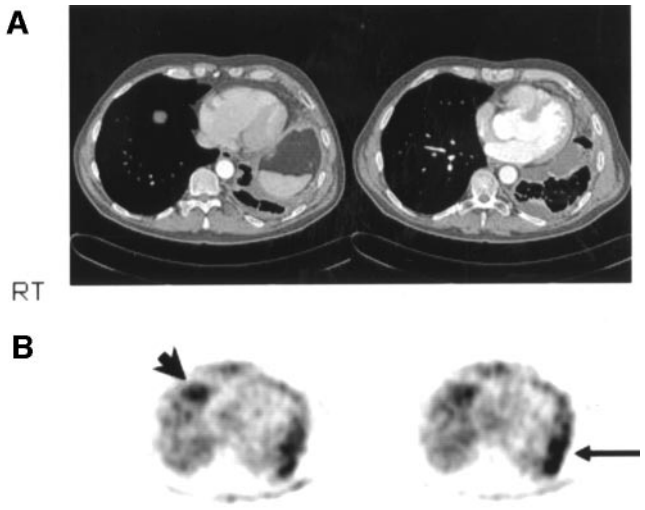

FIGURE 2. (A) Axial CT slices of thorax show circumferential pleural nodularity encasing left hemithorax with volume loss. There is medial loculation of pleural fluid, and pleural effusion is also seen in dependent location at left lung base. There is no evidence of right pleural thickening. RT = right. (B) Axial ^{18}F-FDG-CI shows ^{18}F-FDG hypermetabolism in left pleural cavity (arrow). In addition, there is distinct focus of increased uptake in anterior right costophrenic sulcus suggesting contralateral disease (arrowhead). Histology confirmed bilateral pleural mesothelioma of epithelial type.

with positive ^{18}F-FDG findings in the mediastinum also had extensive transdiaphragmatic and posterior abdominal metastatic disease confirmed by both imaging modalities.

Extrathoracic Metastases and Recurrent Disease

Previously unknown extrathoracic metastatic involvement was shown by ^{18}F-FDG-CI in 5 patients, with biopsy confirmation in 3 and CT confirmation in all 5 patients. Four patients had been treated previously for malignant mesothelioma with trimodality therapy (extrapleural pneumonectomy, chemotherapy, and radiation) (11-mo median and 8- to 30-mo range before ^{18}F-FDG imaging) and 1 patient with partial pleurectomy plus chemotherapy (10 mo before ^{18}F-FDG-CI). All 5 patients had positive intrathoracic and extrathoracic ^{18}F-FDG images confirming local recurrence and distant metastases.

Sites of extrathoracic metastases detected with ^{18}F-FDG imaging included the liver (2 patients), anterior abdominal wall (1 patient), posterior abdominal wall (1 patient), and the peritoneum bilaterally (1 patient) (Fig. 3). These findings constituted the basis for excluding these patients from surgical therapy. The sixth patient being evaluated for recurrence had a negative whole-body ^{18}F-FDG scan and matching CT, with biopsy-proven right chronic fibrosing pleuritis. Extrathoracic metastases were not detected in patients referred for initial staging.

DISCUSSION

The results of this pilot study show that, in the setting of malignant mesothelioma, ^{18}F-FDG-CI is a reliable approach to accurately (a) differentiate malignant from benign disease, (b) evaluate the extent of intrathoracic mesothelioma involvement, and (c) detect the presence of metastatic spread and recurrence.

Eleven of 15 patients had histologically proven malignant mesothelioma, and ^{18}F-FDG imaging was positive in all 11 patients. Thirty-four lesions were biopsied, and ^{18}F-FDG-CI correctly identified 28 of 29 malignant lesions, yielding negative results in 4 of 5 benign lesions. The overall sensitivity, specificity, and accuracy were 97%, 80%, and 94%, respectively. These findings are consistent with those reported by other investigators using full-ring PET technol-

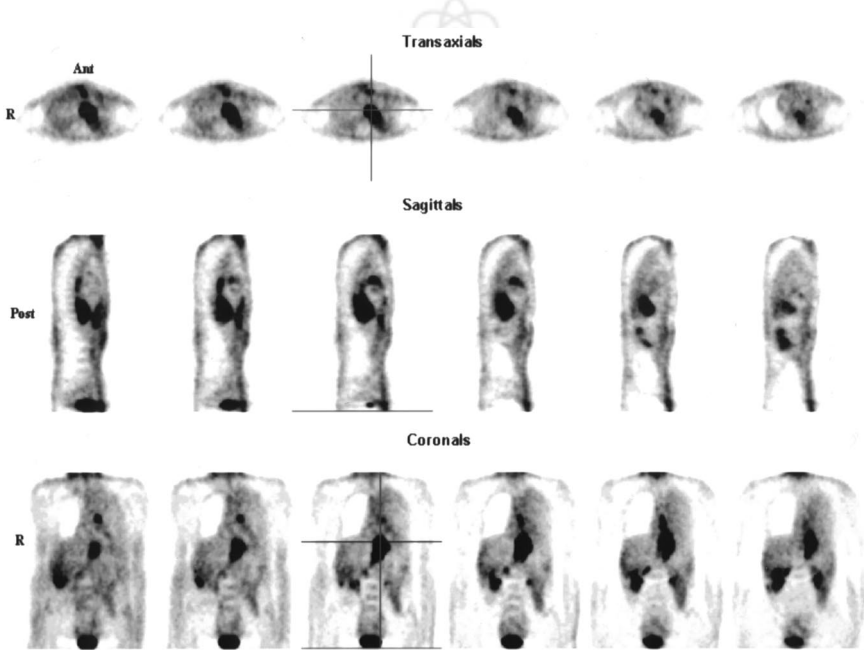

FIGURE 3. ^{18}F-FDG-CI study of patient who had undergone right pleurectomy and chemotherapy for diffuse malignant mesothelioma 18 mo earlier. There is increased ^{18}F-FDG uptake in middle mediastinum extending to posterior mediastinum and to upper-posterior abdomen. In addition, there is abnormal ^{18}F-FDG uptake in superior anterior abdominal wall. Ant = anterior; Post = posterior; R = right.

ogy. Bénard et al. (*7*), using ^{18}F-FDG PET and qualitative analysis, reported a sensitivity of 92%, a specificity of 75%, and an accuracy of 89% for the detection of malignant mesothelioma. These investigators also performed semiquantitative (standardized uptake value [SUV]) measurements in 26 patients. They concluded that using an SUV of >2.0 to differentiate benign from malignant disease, the sensitivity, specificity, and overall accuracy of the method were 91%, 100%, and 92%, respectively. Recently, Schneider et al. (*8*) reported on a retrospective review of 18 consecutive patients with biopsy-proven malignant mesothelioma who underwent ^{18}F-FDG PET at their institution. The authors found that all primary lesions were ^{18}F-FDG avid and that the method proved valuable for distinguishing between benign and malignant pleural disease.

^{18}F-FDG-CI correctly defined the extent of intrathoracic involvement. In our series, 30 of the 34 biopsied lesions were intrathoracic. Of these, 25 were malignant. Seventeen of these 25 lesions involved the pleura, lung parenchyma, or the chest wall. ^{18}F-FDG-CI correctly identified all 17 lesions as malignant and accurately defined the extent of mesothelioma involvement. There was good agreement between ^{18}F-FDG images and surgical findings with respect to tumor resectability. ^{18}F-FDG-CI identified diffuse chest wall involvement in 3 patients, whereas CT was positive only in 1 patient. Contralateral pleural malignancy was confirmed by ^{18}F-FDG-CI in 3 patients, 1 of whom was negative for contralateral disease on CT. The only false-positive result with ^{18}F-FDG-CI was an area of diffuse or low uptake in the right costophrenic sulcus of a patient who had been treated with talc pleurodesis, a standard approach for the treatment of recurrent pleural effusions (*13*). The pleural space is obliterated by inducing a chronic inflammatory response through the instillation of talc, antibiotics, or antiparasitic or chemotherapeutic agents. Increased ^{18}F-FDG uptake has been revealed in a variety of inflammatory processes (*14*–*16*).

In those patients with early-stage disease, the pattern of lesion uptake was usually focal. In those with advanced pleural involvement, the pattern of uptake was linear along the lateral, medial, or basal aspects of the pleura, with or without diffuse extension to the lung parenchyma. Uptake in the lung parenchyma was better distinguished from pleural uptake on the transaxial and sagittal slices than on the coronal views. It was not feasible to differentiate uptake in the parietal pleura from that in the visceral pleura in the absence of a pleural effusion. Similarly, uptake in the basal pleura could not be distinguished from diaphragmatic uptake. Diaphragmatic involvement could be unequivocally diagnosed only when transdiaphragmatic spread was evident.

The remaining 8 malignant thoracic lesions involved the mediastinum of 6 patients. ^{18}F-FDG imaging was positive in 7 lesions (88%) compared with CT, which identified 6 lesions (75%) as malignant. These results should be interpreted with caution in light of the small sample size and the lack of biopsy confirmation in the remaining 5 patients with malignancy. However, our findings compare favorably with those cited in the full-ring PET literature. Bénard et al. (*7*) studied 10 patients with surgical confirmation of lymph node status and reported PET to have a sensitivity of 83% and a specificity of 75% for the detection of lymph node metastases. In our series, 2 of the 7 ^{18}F-FDG–positive lymph nodes were intrapleural (N1) and located in the hilum in 2 patients. Both lesions (1 and 2.8 cm) were highly ^{18}F-FDG avid; however, it was difficult to differentiate them from uptake in the primary tumor. Sugarbaker et al. (*17*) showed that extrapleural (N2) positive nodes are always associated with poor survival. When staging N2 nodes with ^{18}F-FDG-CI, the only false-negative finding was a 0.5-cm tracheobronchial lymph node, with micrometastatic involvement, also reported as negative on CT. The size of this lesion was below the resolution of the ^{18}F-FDG-CI system, and it would have been below the resolution of most dedicated PET scanners. This is an important limitation, and caution should be exercised in this setting. N2 disease, rather than N1 disease, carries the worst prognosis (*18*); therefore, missing even a single node will contribute misleading information with regard to survival and optimal patient management. Thus, invasive techniques are still warranted with a negative mediastinum on ^{18}F-FDG-CI and PET images. In those cases with disease involving mediastinal organs, ^{18}F-FDG uptake was rather diffuse and all-inclusive. It was not possible to distinguish uptake in individual structures. In this setting, ^{18}F-FDG imaging complemented CT and MRI, which provided the fine anatomic detail to identify compromise of each mediastinal structure, accurately predicting unresectability (*5*).

Another important finding was that ^{18}F-FDG imaging correctly defined the presence and extent of extrathoracic disease. ^{18}F-FDG-CI was true-positive in 5 patients with proven extrathoracic metastases, excluding them from extrapleural pneumonectomy. These patients had been referred for ^{18}F-FDG imaging to evaluate for disease recurrence. All patients had local recurrence detected by ^{18}F-FDG as well. All distant metastases were located in the abdomen. The smallest detected lesion was 0.8 cm in its greatest diameter, located in the right lobe of the liver. All metastatic lesions in this series had a higher degree of ^{18}F-FDG avidity compared with that of the primary lesion. ^{18}F-FDG uptake was consistently higher in the primary lesion of patients with distant metastases than in patients without distant disease. These findings expand those of Bénard et al. (*10*), who reported that high ^{18}F-FDG avidity was associated with a poor prognosis in a study cohort of 10 patients with biopsy-proven mesothelioma.

Our preliminary results are promising, but not without certain limitations. Our sample size was relatively small. There was no biopsy confirmation of mediastinal lymph node involvement in 5 patients, 4 of whom were negative and 1 positive on ^{18}F-FDG imaging. More studies comparing ^{18}F-FDG-CI with surgical mediastinal staging are

needed to correctly define the role of CI in the mediastinum of patients with diffuse malignant mesothelioma.

CONCLUSION

These preliminary results provide evidence that ^{18}F-FDG-CI appears to be an accurate method to detect and to define the extent of disease in patients with diffuse malignant mesothelioma.

REFERENCES

1. Spirtas R, Beebe GW, Connelly RR, et al. Recent trends in mesothelioma incidence in the United States. *Am J Ind Med.* 1986;9:397–407.
2. Sugarbaker DJ, Garcia JP, Richards WG, et al. Extrapleural pneumonectomy in the multimodality therapy of malignant pleural mesothelioma: results in 120 consecutive patients. *Ann Surg.* 1996;224:288–296.
3. Sugarbaker DJ, Norberto JJ, Swanson SJ. Surgical staging and work-up of patients with diffuse malignant pleural mesothelioma. *Semin Thorac Cardiovasc Surg.* 1997;9:356–360.
4. Leung AN, Muller NL, Miller RR. CT in differential diagnosis of diffuse pleural disease. *AJR.* 1990;154:487–492.
5. Patz EF Jr, Shaffer K, Piwnica-Worms DR, et al. Malignant pleural mesothelioma: value of CT and MR imaging in predicting resectability. *AJR.* 1992;159: 961–966.
6. Sugarbaker DJ, Norberto JJ, Swanson SJ. Extrapleural pneumonectomy in the setting of multimodality therapy for diffuse malignant pleural mesothelioma. *Semin Thorac Cardiovasc Surg.* 1997;9:373–382.
7. Bénard F, Sterman D, Smith RJ, Kaiser LR, Albelda SM, Alavi A. Metabolic imaging of malignant pleural mesothelioma with fluorodeoxyglucose positron emission tomography. *Chest.* 1998;114:713–722.
8. Schneider DB, Clary-Macy C, Challa S, et al. Positron emission tomography with F18- fluorodeoxyglucose in the staging and preoperative evaluation of malignant pleural mesothelioma. *J Thorac Cardiovasc Surg.* 2000;120:128–133.
9. Carretta A, Landoni C, Melloni G, et al. 18-FDG positron emission tomography in the evaluation of malignant pleural diseases: a pilot study. *Eur J Cardiothorac Surg.* 2000;17:377–383.
10. Bénard F, Sterman D, Smith RJ, Kaiser LR, Albelda SM, Alavi A. Prognostic value of FDG PET imaging in malignant pleural mesothelioma. *J Nucl Med.* 1999;40:1241–1245.
11. Hudson HM, Larkin RS. Accelerated image reconstruction using ordered subsets of projection data. *IEEE Trans Med Imaging.* 1994;13:601–609.
12. Corson JM. Pathology of diffuse malignant pleural mesothelioma. *Semin Thorac Cardiovasc Surg.* 1997;9:347–355.
13. Adler RH, Sayek I. Treatment of malignant pleural effusion: a method using tube thoracostomy and talc. *Ann Thorac Surg*. 1976;22:8–15.
14. Strauss LG. Fluorine-18 deoxyglucose and false-positive results: a major problem in the diagnostics of oncological patients. *Eur J Nucl Med.* 1996;23:1409–1415.
15. Zhuang H, Pourdehnad M, Lambright ES, et al. Dual time point ^{18}F-FDG PET imaging for differentiating malignant from inflammatory processes. *J Nucl Med.* 2001;42:1412–1417.
16. Alavi A, Zhuang H. Finding infection: help from PET [commentary]. *Lancet.* 2001;27:1386.
17. Sugarbaker DJ, Flores RM, Jaklitsch MT, et al. Resection margins, extrapleural nodal status, and cell type determine postoperative long-term survival in trimodality therapy of malignant pleural mesothelioma: results in 183 patients. *J Thorac Cardiovasc Surg.* 1999;117:54–65.
18. Sugarbaker DJ, Strauss GM, Lynch TJ, et al. Node status has prognostic significance in the multimodality therapy of diffuse, malignant mesothelioma. *J Clin Oncol.* 1993;11:1172–1178.